Supplementary discussion

Spatial confinement

Here we discuss the parameters that determine the dimensions of the sound modulation zone. The transverse confinement is determined by the focusing parameters of the sound transducer. The transducer's (Olympus NDT v3330) element diameter and focal length are 0.25 inch and 0.2 inch, respectively. The ideal full width half maxim (FWHM) of the sound focus should be $1.02F\lambda/D$, where F is the focal length, λ is the sound wavelength and D is the element diameter. For a 50 MHz sound wave in water (sound velocity 1500 m/sec), the ideal FWHM is 24.5 microns. Supplementary Fig. 7 **a** shows the measured dependence of the sound modulated light power on the driving voltage of the sound transducer. With low (< 50 V) driving voltage, the modulated light power shows a quadratic dependence on driving voltage or a linear dependence on the driving power ($\propto V^2$). In experiments, we used high (140-160 V_{p-p}) driving signal to achieve good modulation efficiency. With high driving voltage, the signal approaches linear dependence on the driving voltage, making the sound modulation zone larger than the sound focus. In addition, the driving signal is a 20 ns single cycle sinusoidal pulse, as shown in Supplementary Fig. 7 **c**. Its Fourier transform (Supplementary Fig. 7 **e**) contains a broad bandwidth including lower frequency longer wavelength sound waves, which makes the focus larger than the value calculated with 50 MHz sound wave. The axial confinement is determined by the speed of sound, the sound pulse duration and the laser pulse duration. For laser pulses much shorter than 20 ns, the sound pulse position hardly changes during laser illumination and the axial confinement approximately equals the sound pulse duration multiplied by the speed of sound. In experiments, the laser pulse FWHM duration is 20 ns (Supplementary Fig. 7 **b**). During laser illumination, the sound pulse travels and the axial confinement is therefore the

speed of sound multiplied by the sound pulse duration convolved with the laser illumination time. Supplementary Figure 7 **d** is the convolution of Supplementary Fig. 7 **b** with the amplitude of Supplementary Fig. 7 **c**. The FWHM of Supplementary Fig. 7 **d** is 25.5 ns and the axial confinement is therefore 38.4 microns, which is close to the measured 37.9±2.3 microns.

SNR and speed considerations

Let's assume that during the sound modulation, the CMOS camera receives u photons of light from the sample, among which cu photons are sound modulated. c is a coefficient ($<<1$) that depends on the sound modulation efficiency (~1%), the thickness and the scattering property of the tissues. We interfere the sample light with v photons of reference light. The interference signal is therefore $2\sqrt{cuv}$. Experimentally, the signal level of the CMOS camera is near its full well charge capacity and therefore the noise is dominated by the shot noise from the light ($\sqrt{u+v}$). The SNR is $2\sqrt{cuv}/\sqrt{u+v}$. For a given time, the maximum number of photons the CMOS camera can collect is wf, where w is the full well charge capacity and f is the number of frames. We need to maximize $2\sqrt{cuv}/\sqrt{u+v}$ under the condition that $u+v \le wf$. The maximum SNR is $\sqrt{cwf}$, which is achieved when $u=v=wf/2$. Experimentally, we control the light power such that the sample light and reference light have similar power and the total power is close but less than the full well limit. Our CMOS camera has a full well charge capacity of 90,000e- and it runs at 40 frames per second. Employing cameras with higher full well charge capacity and frame rate can potentially accelerate the measurements.

Speckle correlation measurement

To measure the correlation length in the samples, the following approach was used: CW laser light (778nm wavelength) was focused with an Olympus NA 1.2/60X water immersion objective onto the sample. The emerging speckle pattern on the backside of the sample was imaged with an Olympus NA 0.75/40x air objective onto a CCD camera. In the measurement, the sample was translated with a piezo stage and at each position an image of the speckle pattern was acquired. In the post-processing, a normalized cross-correlation between the middle image and all other images was computed. The correlation coefficient was extracted and fitted with a Gaussian curve, as shown in supplementary Fig. 8.

Tissue phantom preparation and scattering coefficient measurements

A polystyrene bead suspension was dispersed in agar (1.5 % in H_2O). The sample was mixed on a shaker until it appeared uniform. Specially made metal spacers were sandwiched between two pieces of cover glass to control the phantom's thickness. The polystyrene beads in agar mixture was then injected between the cover glass to create tissue phantoms. 1.5 micron diameter polystyrene beads suspension (2.61%) was mixed with agar at 33:467 volume ratio for the tissue phantoms used for Fig. 2, 3 and Supplementary Fig. 1. The scattering anisotropy parameter (g factor) is 0.9306 based on Mie scattering calculation[1] (we used $n_{water} = 1.330$ and $n_{polystyrene} = 1.579$). 1.0 micron diameter bead suspension (2.6% solid) was mixed with agar at 1:9 and 3:37 volume ratio for the tissue phantom used for Supplementary Fig. 3 and 5, respectively. The calculated g factor is 0.9013. To measure the scattering coefficient, we used a collimated laser beam (centered at 780nm) to illuminate the sample. We measured the ballistic component of the transmitted light at ~ two meters distance from the tissue phantom. For this measurement, we used tissue phantoms of thickness 0.2, 0.4, 0.6, 0.8 and 1 mm and rat brain slices of thickness 0.1, 0.2, 0.3, 0.4 and 0.5 mm. For each thickness, multiple phantoms were prepared and two rat brain

slices were used. For each phantom, we repeated the measurement at three different positions of the phantom. For the rat brain slices, the laser beam was carefully positioned on areas void of white matter and a measurement was performed for at least three positions. The experimental data was fitted with an exponential curve to determine the scattering coefficient and the 95% confidence bounds, as shown in supplementary Fig. 9.

FBR estimation

There are 1920 x 1080 pixels on the SLM. In the current implementation, we arranged the optical signal collection such that one speckle occupies ~2x2 pixels on the SLM to reduce the phase errors due to pixel-to-pixel phase coupling. In addition, the SLM has limited filling factor and diffraction efficiency, and temporal phase fluctuation[2]. We tested our DOPC system using a collimated laser beam as the input ($N_{mode} = 1$) and a stack of three glass diffusers (Thorlabs DG10-120, DG10-220, and DG10-600) as the scattering media. The FBR of the phase conjugated beam reached ~40,000. We performed speckle correlation measurements to quantify the spatial correlation length through the three different tissue phantoms and the brain slices used in our experiments. The results are summarized in Supplementary Fig. 8. The typical correlation length in our experiments is ~0.42 micron. We estimate the FBR to be $\sim 40{,}000/2/(38/0.42)^2 = 2.4$, which is of the same order as the observed values (1.5-4). Here the number 38 corresponds to the FWHM of the PSF along y and z directions in our experiments. We would like to note that in this approximation the sound light interaction was assumed to happen in a 2D cross-section of the sound focus. In reality the interaction is happening in a 3D Volume, potentially giving rise to even more modes. The factor 2 originates from the two possible polarization states.

Iterative Ultrasound guided DOPC

In the current implementation, we have no control of the wavefront of the illumination light during the sound modulation. We can potentially employ two DOPC systems and let them take turns to illuminate the sample during sound modulation and to record the sound modulated light. In such a way, the illumination light during sound modulation no longer randomly diffuses in the scattering media. Instead, an optical focus is formed at the sound focus. Through multiple iterations, we can potentially achieve a much smaller sound light interaction volume, leading to not only better spatial resolution but also higher FBR due to the reduced N_{mode}. We are currently developing this technique.

Supplementary References

1. Prahl, S. Mie Scattering Calculator http://omlc.ogi.edu/calc/mie_calc.html.
2. Lizana, A. et al. Time fluctuations of the phase modulation in a liquid crystal on silicon display: characterization and effects in diffractive optics. *Optics Express* **16**, 16711-16722 (2008).

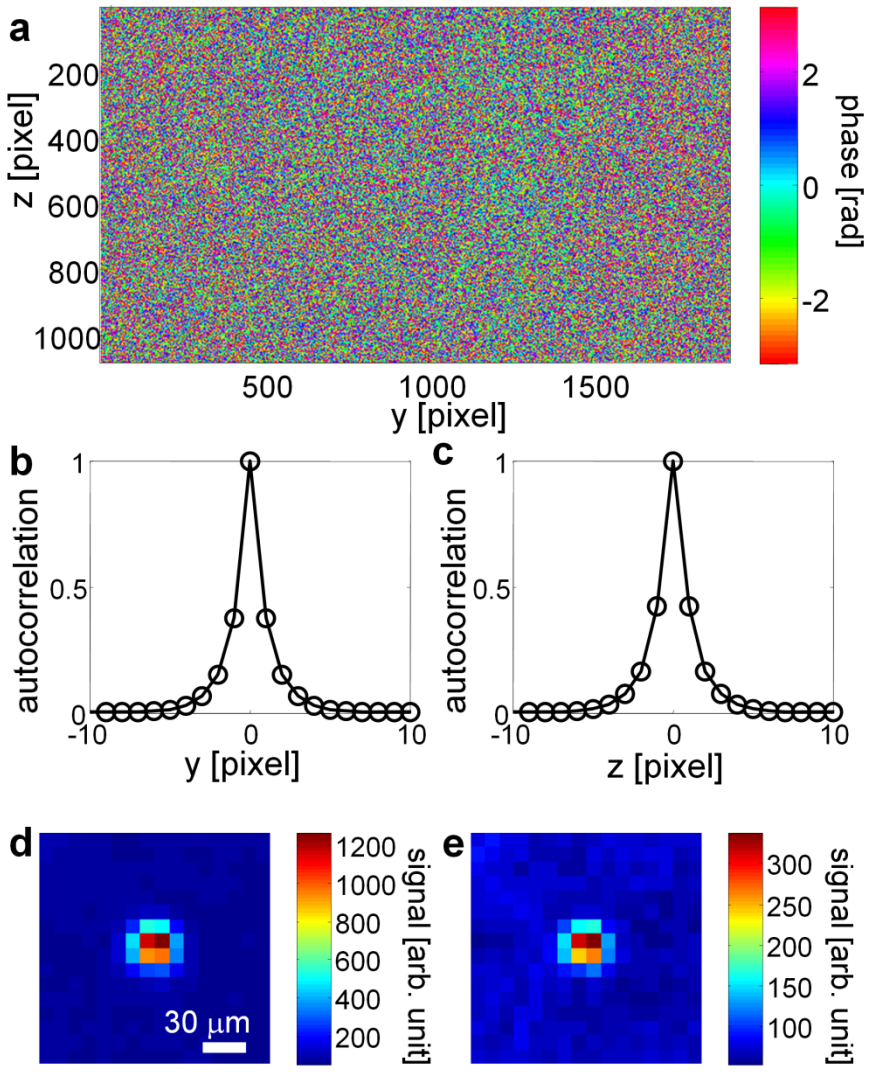

Supplementary Figure 1

a One of the phase patterns $p(y,z)$ used for phase conjugation. **b** and **c** are the autocorrelations of wavefront $\exp(ip(y,z))$ along y and z directions, respectively. A small displacement makes the OPC ineffective. **d** Direct widefield image of one fluorescence bead illuminated by the OPC beam through a 2 mm thick tissue phantom (μ_s=6.42/mm, g=0.9306). **e** Direct widefield image of the bead after the phase pattern was shifted on the SLM (making OPC ineffective). The units in **d** and **e** are identical. The signal ratio between **d** and **e** is 3.7.

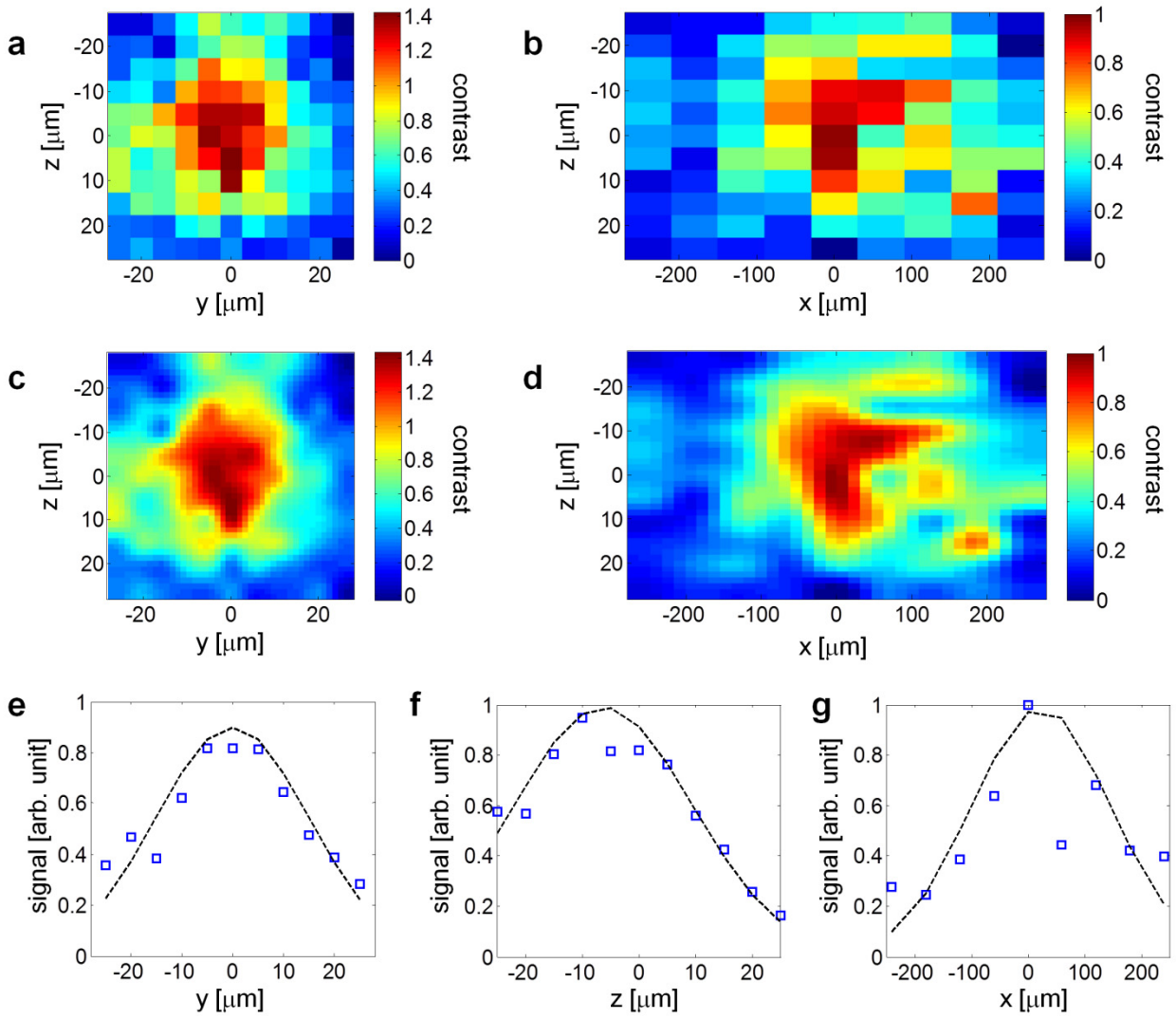

Supplementary Figure 2

PSF measurement through 1.2 mm thick fixed rat brain slices. 6 microns diameter beads dispersed in 1 mm thick agar slice were sandwiched by two 1.2 mm thick brain slices **a**, Measured transverse PSF. **b**, Measured axial PSF. **c** and **d** are the corresponding images resampled with bicubic interpolation. **e-g**, the cross-section of the PSF with Gaussian fitting. The FWHM in y, z, and x are 35.6±4.7, 35.5±4.6, and 288±99 microns (95% confidence bound).

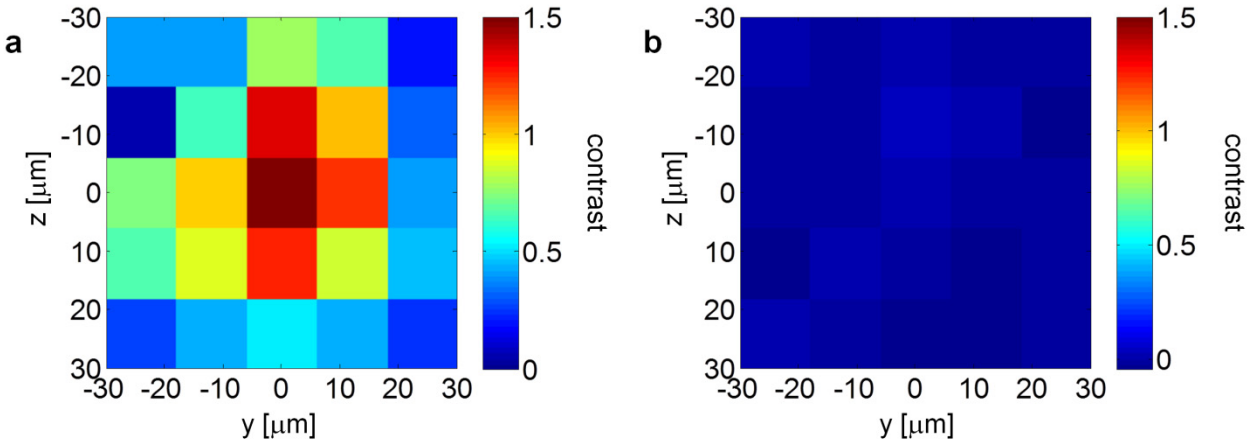

Supplementary Figure 3

a Transverse PSF measured through 2mm thick tissue phantoms (g=0.9013, μ_s=10.5/mm) with the ultrasound transducer's amplifier on. **b** The same measurement with the amplifier off.

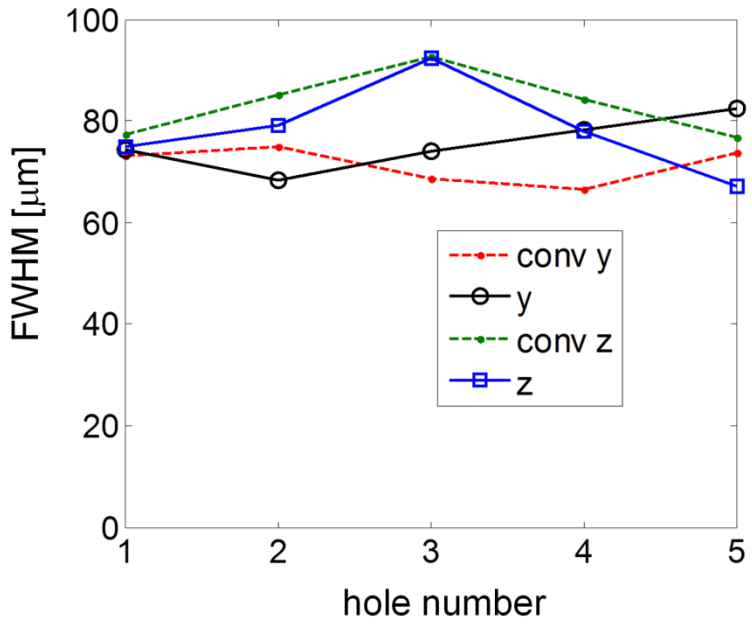

Supplementary Figure 4

Full width half maximum of the fluorescence holes obtained by 2D Gaussian fitting (hole 1-5, top to bottom) in Fig. 3 **d** (y, z) and **e** (conv y and z).

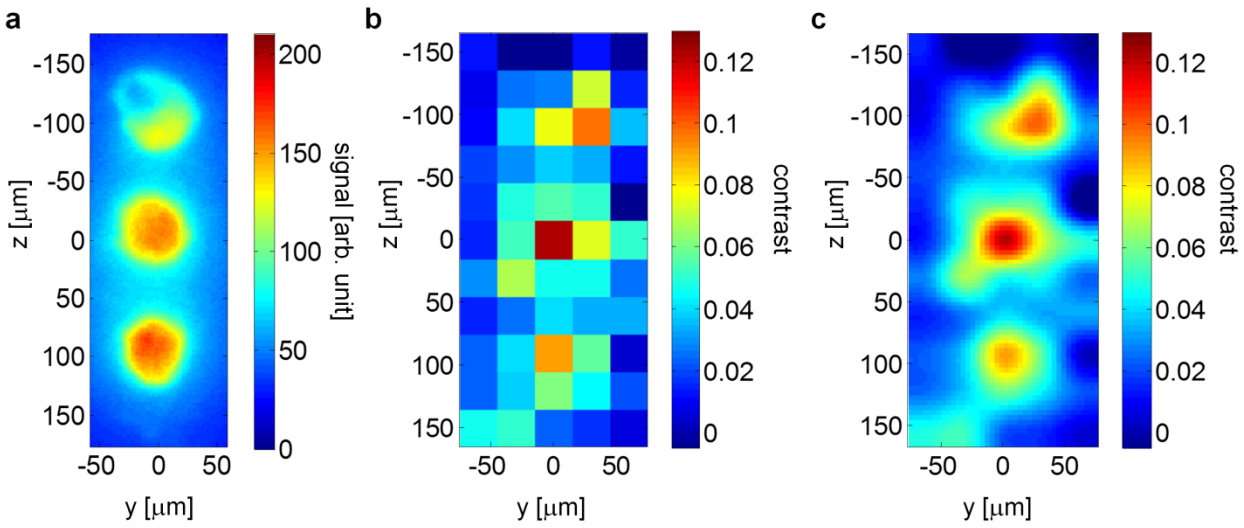

Supplementary Figure 5

a Direct wide field fluorescence image of the hole array that was directly created on the surface of a 2 mm thick tissue phantom. After this wide field image was recorded, a second 2 mm thick tissue phantom was added such that the fluorescence features were completely embedded in the middle of the 4 mm thick scattering medium (g=0.9013, μ_s=7.09/mm). **b** Image acquired with ultrasound pulse guided DOPC through the closed tissue phantom. **c** The image in **b** resampled with bicubic interpolation.

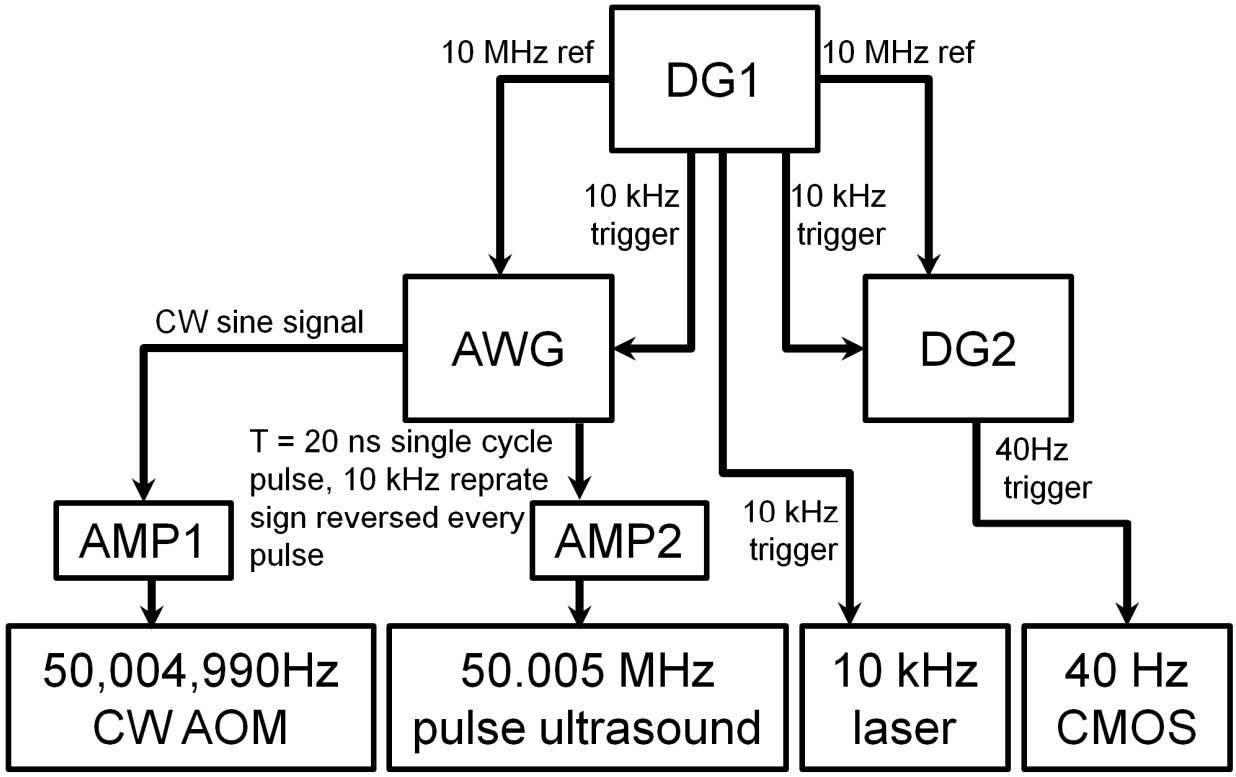

Supplementary Figure 6

Timing and synchronization diagram. DG1, delay generator (Stanford Research DG645); AWG, arbitrary waveform generator (Tektronix AFG3252); DG2, delay generator (Stanford Research DG535); AMP1, RF amplifier (AR, 75A250A); AMP2, RF amplifier (AR, 25A250A).

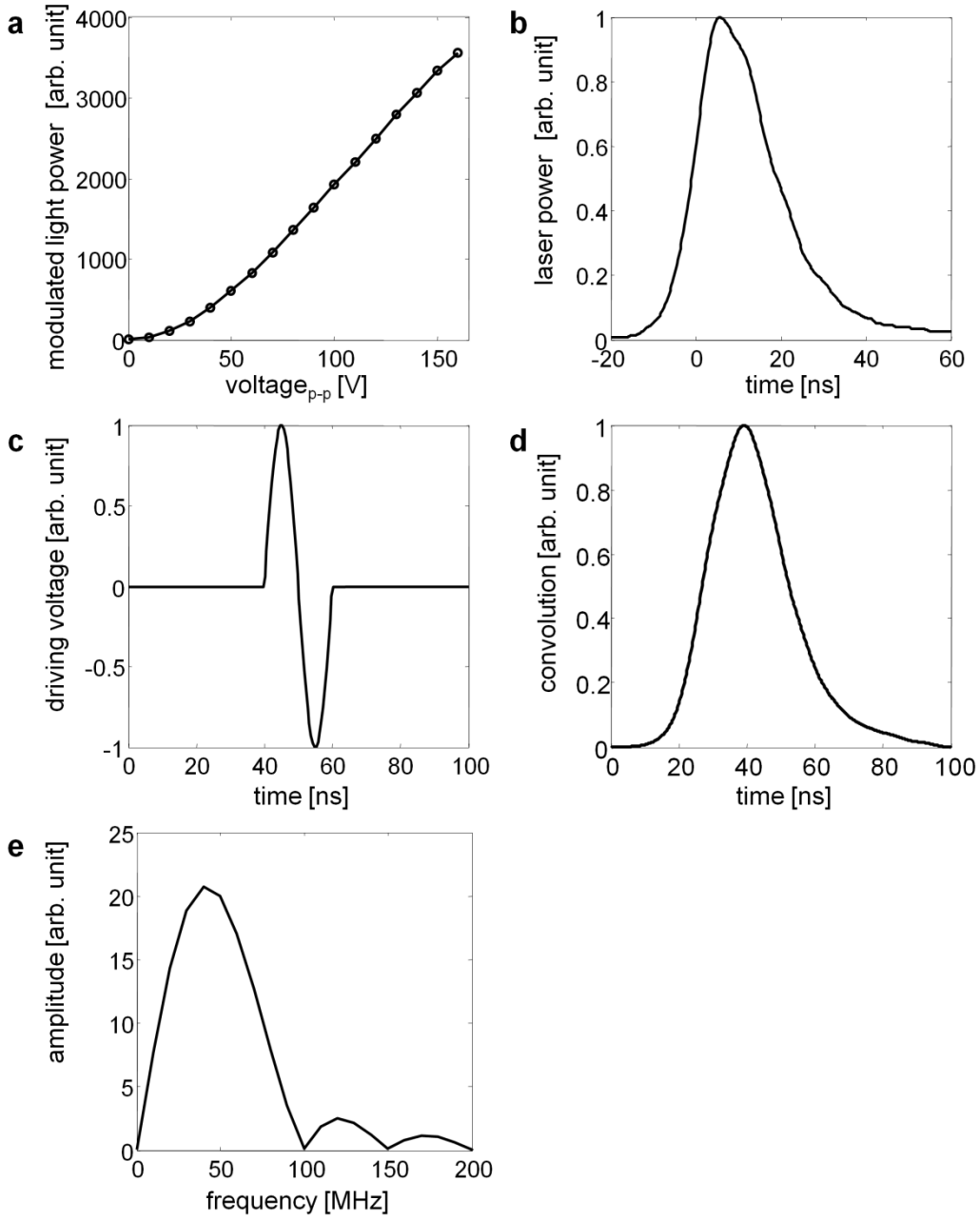

Supplementary Figure 7

a Dependence of the modulated light power on the driving voltage of the ultrasound transducer. **b** Measured temporal profile of the laser pulse. **c** Single cycle sinusoidal pulse used for driving the ultrasound transducer. **d** Convolution of **b** and the amplitude of **c**. **e** Fourier transform of **c**.

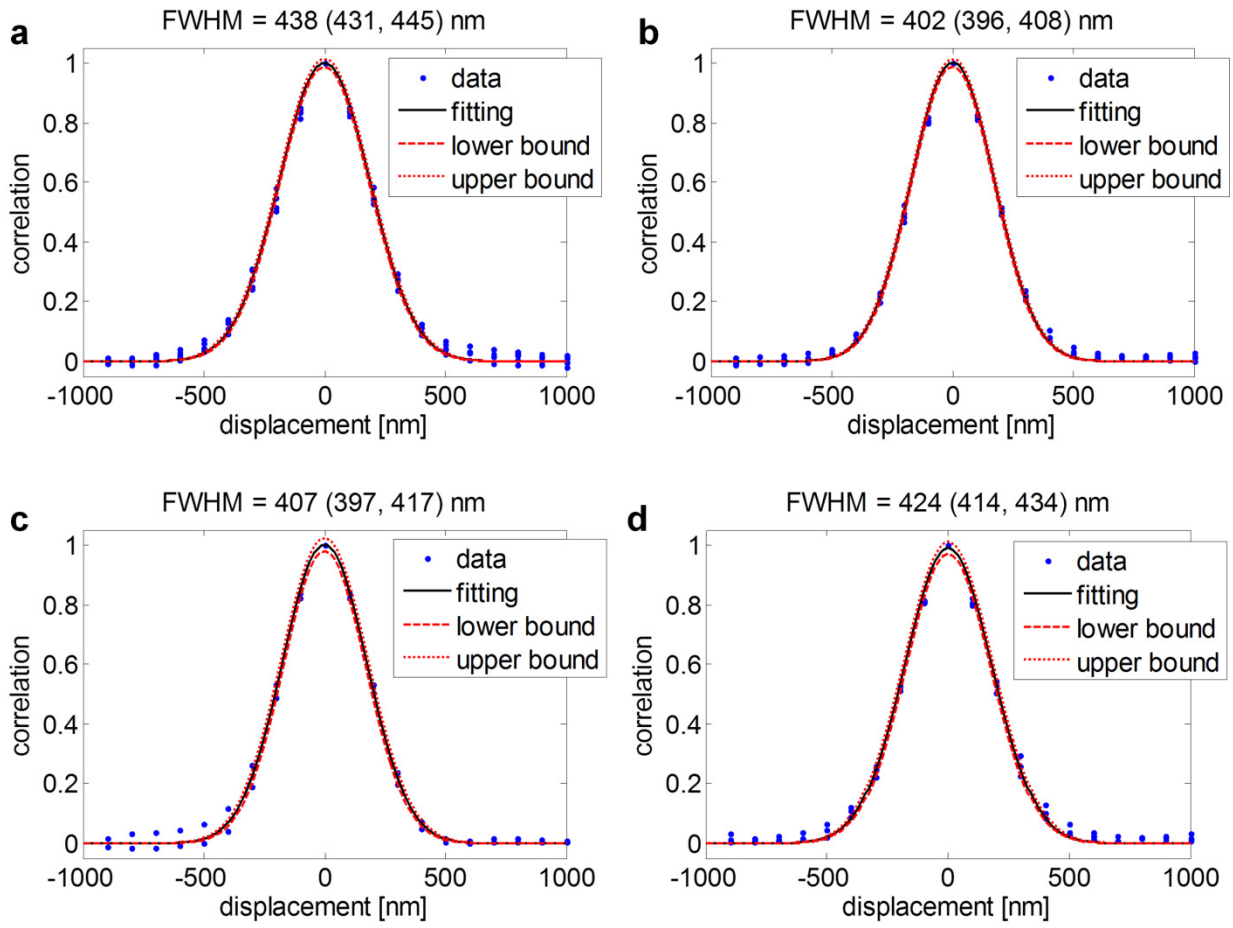

Supplementary Figure 8

Speckle correlation measurements for four samples: **a**, 1.5 micron diameter polystyrene bead suspension (2.61% solid) + agar at 33:467 volume ratio, 2 mm thick; **b**, 1 micron diameter polystyrene bead suspension (2.6% solid) + agar at 1:9 volume ratio, 2 mm thick; **c**, 1 micron diameter polystyrene bead suspension (2.6% solid) + agar at 3:37 volume ratio, 2 mm thick; **d**, 1.2 mm thick fixed rat brain (cortex area). The Gaussian fitting (solid dark line), the 95% confidence lower bound (red dashed line) and upper bound (red dotted line) are also shown.

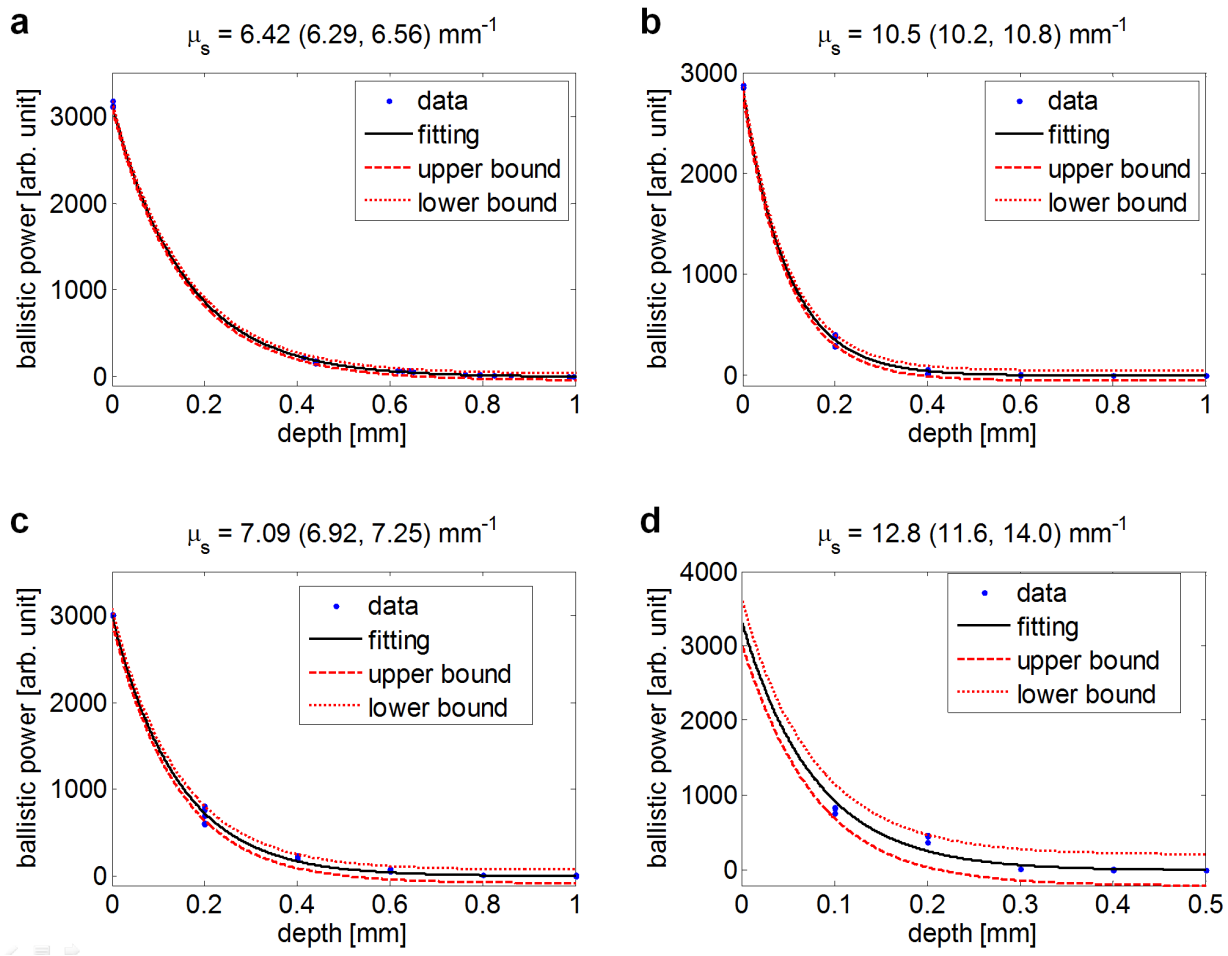

Supplementary Figure 9

The scattering coefficient measurements of four samples: **a**, 1.5 micron diameter polystyrene bead suspension (2.61% solid) + agar at 33:467 volume ratio; **b**, 1 micron diameter polystyrene bead suspension (2.6% solid) + agar at 1:9 volume ratio; **c**, 1 micron diameter polystyrene bead suspension (2.6% solid) + agar at 3:37 volume ratio; **d**, fixed rat brain (cortex area). The exponential fitting (solid dark line), the 95% confidence upper bound (red dashed line) and lower bound (red dotted line) are also shown.